Stimuli-Responsive Epoxy Coatings

Liming Tang,[†] John Whalen,[†] Grant Schutte,[†] and Christoph Weder*[,†,§]

Departments of Macromolecular Science and Engineering and of Chemistry, Case Western Reserve University, 2100 Adelbert Road, Cleveland, Ohio 44106-7202, and The Valspar Corporation, 2001 Tracy Street, Pittsburgh, Pennsylvania 15233

ABSTRACT The design, formulation, and characterization of new epoxy coatings with built-in chemical and threshold temperature sensors are reported. The materials were prepared by dissolving a chromogenic, fluorescent oligo(p-phenylenevinylene) dye into a cross-linked epoxy resin by reacting monomer/cross-linker/dye mixtures at 180−200 °C and quenching the cured polymer to below its glass transition temperature (T_g). Subjecting these kinetically trapped, thermodynamically unstable molecularly mixed epoxy/dye blends to temperatures above T_g leads to aggregation of the dye molecules and causes permanent and pronounced changes of their optical absorption and fluorescence properties. Exposure of the materials to selected chemical stimuli, e.g., water, acid, base, and several organic compounds, also causes plasticization of the polymer matrix and leads to irreversible aggregation of dye molecules, concomitant with the pronounced fluorescence and absorption color change. This response is well described by standard kinetic models and can be controlled via the chemical structure and cross-link density of the resin and the dye content.

KEYWORDS: coating • color change • epoxy resin • fluorescent sensor • stimuli-responsive

INTRODUCTION

Significant attention has been devoted in the past years to the development and investigation of chromogenic polymers, which have the ability to change their absorption and/or fluorescence properties in response to external stimuli such as heat (1−7), deformation (8−12), light (13−15), or chemicals (16−23). Such stimuli-responsive materials are of great interest for a wide range of sensor applications (24). We recently introduced a novel approach for the design of polymers with built-in mechanical (25−29), temperature history (30−35), and humidity (36) sensors. The operating principle of our thermoresponsive materials relies on the phase separation of initially molecularly mixed blends of excimer-forming or aggregachromic (32) dyes and glassy amorphous or semicrystalline host polymers (31, 33). These mixtures are produced by incorporating small quantities of the chromophores into the host polymer via melt-processing and quenching of these materials from a homogeneous melt to below their glass transition temperature (T_g). Heating these kinetically trapped, thermodynamically unstable molecular mixtures to temperatures above their T_gs leads to aggregation of the dye molecules, concomitant with a permanent change of fluorescence and/or absorption properties. Because the aggregation kinetics follow a predictable Arrhenius-type behavior (31−33), the sensory performance is very useful in the fabrication of threshold temperature or time−temperature indicators. A similar approach for humidity sensors exploits the plasticization effect of water on a hygroscopic polymer (36). In this case, exposure to water causes a decrease of T_g and causes aggregation of the initially dispersed sensor molecules.

Previous studies by our group (25−36) and others (37−40) were limited to the exploitation of the aggregachromic sensor approach in thermoplastic polymers. We here report on the adaptation of the framework to an epoxy-based, thermosetting resin, as an example for a reactive polymer system with integrated sensing capabilities. Such resins are widely used for decorative, protective, and/or functional coatings (41). Protective epoxy coatings are used in many industries because of their excellent chemical resistance, tenacious adhesion, and toughness (42). The coating not only provides mechanical protection of the underlying substrate but also acts as a chemical barrier. The coating's properties can be compromised by exposure to excessive heat or penetrating chemicals; therefore, the integration of sensing capabilities into such materials is of significant technological interest. Through a systematic study of a relevant model system, we unequivocally demonstrate that multifunctional thermoset epoxy coatings with thermal and chemical sensing capabilities can be designed on the basis of the aggregachromic sensor approach.

EXPERIMENTAL SECTION

Materials. 1,4-Bis(α-cyano-4-octadecyloxystyryl)-2,5-dimethoxybenzene (C18-RG; Figure 1) was prepared as previously described (31). An oligomeric difunctional diglycidyl ether of bisphenol A (DGEBA) with an epoxide equivalent weight of 1700−2300 and a T_g of 80 °C and a 60% (w/w) solution of a pyrimidine-based urea-formaldehyde (UF) cross-linker in butyl cellosolve (Beetle 1052-8; Figure 1) were obtained from Hexion Specialty Chemicals, Inc., and Cytec Industries Inc., respectively. All solvents employed were of analytical grade and were purchased from Fisher Science Inc. White distilled vinegar (Crowning Food, 5% acidity), Swiss plum liquor [Etter Kleines Pflümli 41% (v/v)], aftershave (Calvin Klein Obsession for Men), aviation hydraulic fluid (Skydrol 5), and brake fluid (Advance
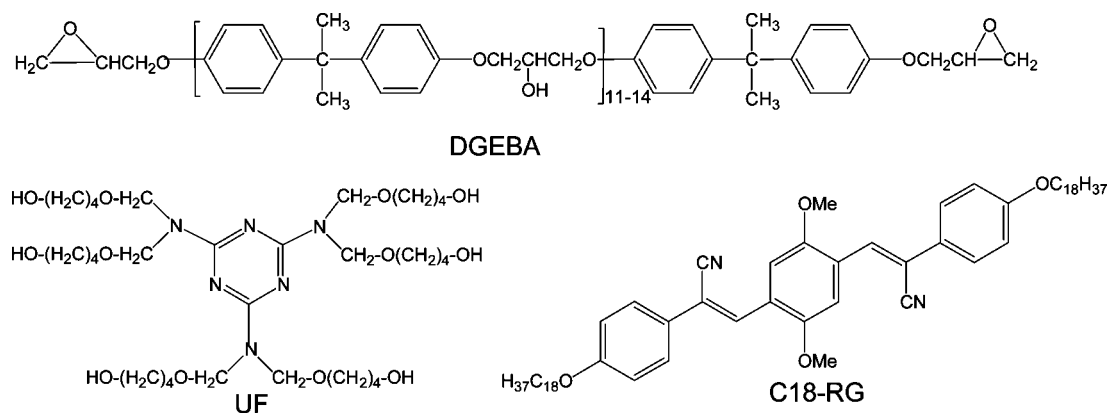
FIGURE 1. Chemical structures of DGEBA and the UF cross-linker used as a basis for the epoxy resins investigated and the chromogenic oligo(*p*-phenylenevinylene) dye (C18-RG) employed in this study.
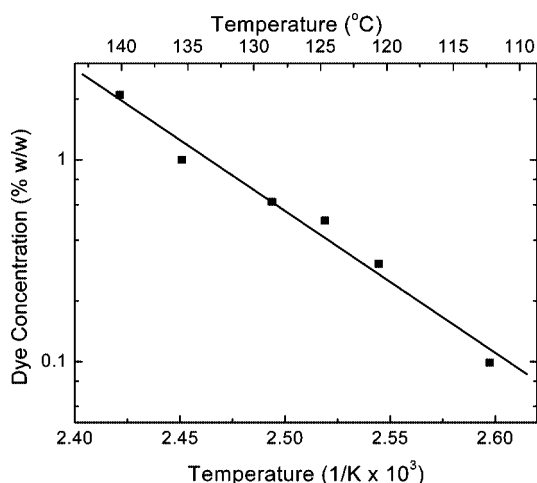

FIGURE 2. Solubility of C18-RG in uncured 100:25 (w/w) DGEBA/UF mixtures as a function of the temperature.

Auto Parts), all used for the experiments shown in Figures 9 and S8 in the Supporting Information, were purchased from retailers.

General Procedure for Preparation of Coatings. A 100:25:1 (w/w/w) DGEBA/UF/C18-RG coating was produced as follows: DGEBA (4.00 g) was dissolved at 100 °C in 4.00 g of butyl cellosolve. C18-RG (40 mg) was dispersed in 7.009 g of methyl ethyl ketone (MEK) by sonicating for 6 h at room temperature. The dye dispersion was added to the DGEBA solution, and 1.667 g of a 60 % (w/w) solution of the UF cross-linker was added. The mixture was then stirred at room temperature until C18-RG was evenly dispersed, typically for 5 min. An aliquot of the mixture was then placed onto a microscope slide, and a uniform film was produced by spreading the mixture with a size 8 wire-wound drawdown bar as described in ASTM D4147-99. The samples were then placed on a Gel Instrument AG hot stage on which they were cured for 10 min (unless otherwise noted) at the desired temperature between 180 and 200 °C; they were subsequently cooled to room temperature by removing them from the hot stage and placing them quickly onto the counter-top, which was used as a heat sink. The thickness of the coatings thus produced, measured with a digital caliper, was in the range of 8−10 μm. Films of other compositions were produced in a similar fashion.

Instrumentation. Differential scanning calorimetry (DSC) experiments were conducted under N_2 on a Perkin-Elmer DSC Pyris 1 at heating and cooling rates of 10 °C min^{-1}. Samples (scraped off the glass slides on which they were cured) were cycled from 25 to 100 °C and back and were then heated to 250 °C. The reported T_gs of cross-linked materials were determined from the second heating scans. UV−vis absorption

spectra were obtained on a Perkin-Elmer Lambda 800 spectrometer at ambient temperature. Steady-state photoluminescence (PL) spectra were acquired at ambient temperature on a PTI C720 spectrometer under excitation (λ_{ex}) at 435 nm (the emission was corrected for instrument throughput and detector response) or in situ on an Ocean Optics ACD1000-USB spectrometer ($\lambda_{ex} = 377$ nm, emission uncorrected). Temperature-dependent PL experiments were conducted by placing samples on a Gel Instrument AG hot stage in connection with a TC2 temperature controller, and the PL spectra were measured with the Ocean Optics ACD1000-USB spectrometer by making use of a Y-shape optical fiber. The same setup was used for solubility tests and immersion studies. For the solubility measurements, samples were spread onto glass slides by the procedure outlined above and dried overnight at ambient temperature. They were subsequently heated on the hot stage and allowed to equilibrate at a specified temperature for 10 min; PL emission spectra were recorded, the temperature was increased, and the process was repeated. For the immersion experiments, cured samples were placed in a Petri dish that was filled with ethanol and in situ PL experiments were carried out while the sample was submerged in the solvent, except for 100:12.5:3 (w/w/w) DGEBA/UF/C18-RG blends, where the samples were removed periodically and were measured using the PTI spectrometer.

RESULTS AND DISCUSSION

The resin systems used in the present study comprised DGEBA with an epoxide equivalent weight of 1700−2300 and the pyrimidine-based UF cross-linker Beetle 1052-8 as a curing agent (Figure 1). C18-RG (Figure 1) was used as the sensor dye. This chromophore is a chromogenic cyano-substituted oligo(*p*-phenylenevinylene) derivate (cyano-OPV). Members of this chromophore family are excellent candidates for use in the sensory scheme exploited here, thanks to their pronounced tendency for excimer formation, their extremely large red shift when comparing excimer to monomer, their high thermal stability, and the ease with which they can be tailored to adjust their solubility in the polymeric host (43, 44). The hydrophobic octadecyloxy chains make C18-RG particularly useful because they impart insolubility in polar host polymers (31) and rapid aggregation kinetics (27). Scouting experiments (data not shown) confirmed that 1,4-bis(α-cyano-4-dodecyloxystyryl)-2,5-dimethoxybenzene (31) displays very similar aggregation characteristics in the epoxy resins investigated here. A detailed description of the optical properties of C18-RG is given elsewhere (31). The UV−vis absorption spectrum of C18-
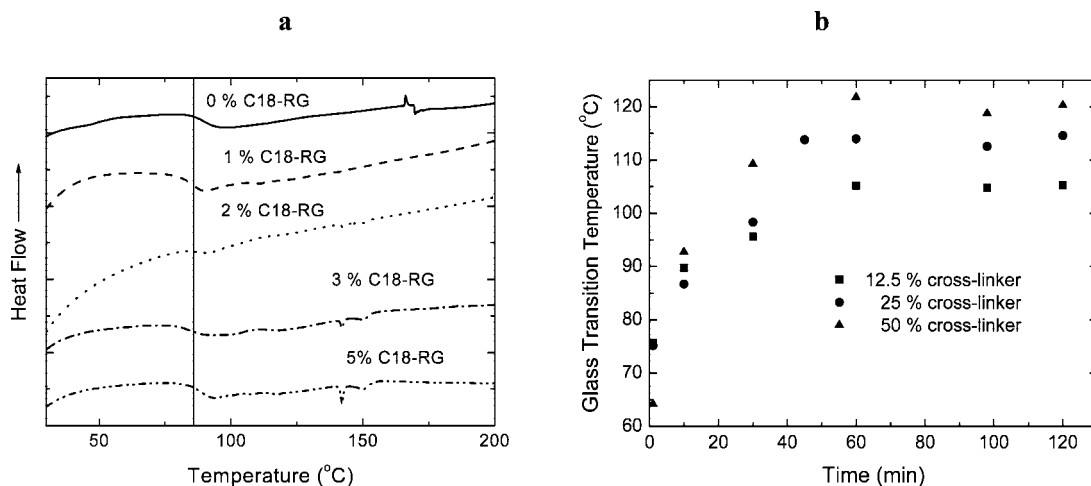
a

b

FIGURE 3. (a) DSC traces of DGEBA/UF resins [100:25 (w/w)] containing 0−5% (w/w) C18-RG. The samples were cured for 10 min at 200 °C, and second heating scans, recorded at heating rates of 10 °C min^{-1}, are shown. The vertical line indicates the common T_g of 86 °C. (b) Plot of T_g (determined from the second heating scans of DSC traces; see the Supporting Information) as a function of the curing time at 200 °C for DGEBA/UF blends comprising 1% (w/w) C18-RG and 12.5% (w/w) (■), 25% (w/w) (●), or 50% (w/w) (▲) UF.
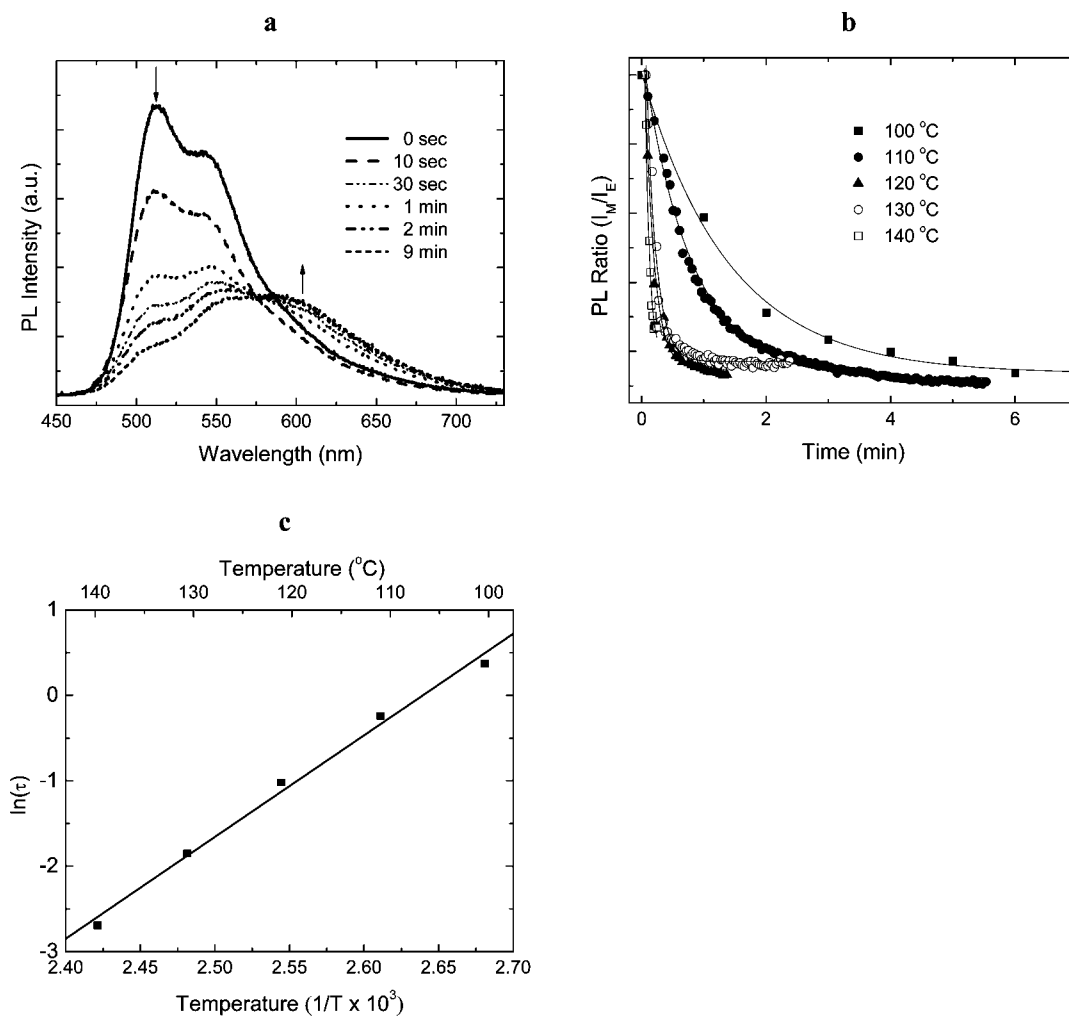
a

b

c

FIGURE 4. (a) Uncorrected PL emission spectra of 100:25:3 (w/w/w) DGEBA/UF/C18-RG coatings (cured for 10 min at 200 °C) as a function of the annealing time at 120 °C. (b) Relative intensities of monomer-to-excimer emission I_M/I_E extracted from the spectra shown in part a as a function of the annealing time (▲). Also shown are data obtained in a similar manner for the same composition annealed at 100 °C (■), 110 °C (●), 130 °C (○), and 140 °C (□). Solid lines are least-squares fits according to eq 1. (c) Plot of ln(τ), extracted from the fits shown in part b against the inverse annealing temperature 1/T.

RG in CHCl$_3$ displays a maximum at 434 nm, and the solution fluoresces green with emission maxima at 507 and

538 nm. The introduction of methanol (a nonsolvent, which causes dye aggregation) shifts the absorption maximum to

380 nm and triggers a new, weak shoulder around 493 nm, owing to charge-transfer interactions as well as conformational changes that increase the highest occupied molecular orbital−lowest unoccupied molecular orbital gap (32). At the same time, the addition of methanol results in a pronounced bathochromic shift of the fluorescence (maximum at 644 nm) due to the formation of excimers. Previous experiments indicated that photooxidation of the dye may occur if exposed to air at high temperature for extended periods of time (35). Under the conditions used here (vide infra), no photodegradation was evident.

In order to elucidate the phase behavior of the resin/sensor dye system, the solubility of C18-RG in DGEBA/UF was investigated in the temperature regime between 25 and 140 °C using in situ PL spectroscopy. For this purpose, 100:25 (w/w) mixtures of DGEBA/UF comprising between 0.1 and 2% (w/w) C18-RG (all dye concentrations are given relative to DGEBA) were solution-cast from a mixture of butyl cellosolve and MEK and dried overnight at ambient temperature, i.e., under conditions that prevented curing of the resin. Upon excitation with UV light, the blend films thus produced exhibit red fluorescence, characteristics of excimer aggregates. The uncured, phase-separated films were subsequently heated; the temperature was increased in increments of 10 °C, and the samples were kept at each temperature for at least 10 min. PL spectra were recorded, and the temperature at which the excimer emission disappeared indicated that the dye had been molecularly dissolved in the host polymer. The inverse dissolution temperatures thus determined were plotted against the logarithmic dye concentration (Figure 2). The observed linear relationship between the logarithm of the dye concentration and $1/T$ is in agreement with the theoretical description for the dissolution of crystalline additives in amorphous polymers (45, 46) as well as with our previous findings for the solubility of this dye in polyethylene (28) and poly(ethylene terephthalate glycol) (31). Importantly, the data show that, for the entire composition range investigated [0.1−2% (w/w) dye (47)], C18-RG is thermodynamically soluble in the monomer mixture at 180−200 °C (i.e., the curing temperature range employed vide infra) but phase-separates under thermodynamic control from the resin at temperatures below 140−110 °C.

Coatings of the dye-containing resin system were produced by spreading solutions comprising DGEBA, UF [12.5, 25, or 50% (w/w) relative to DGEBA], and C18-RG [0.5−5% (w/w)] onto glass substrates and curing the films at 180 or 200 °C for between 10 and 180 min. After curing, the samples were always quenched to room temperature in order to kinetically trap molecularly dispersed dye/resin mixtures and prevent aggregation of the dye molecules. Indeed, all coatings thus prepared fluoresce green upon excitation with UV light and display emission spectra characteristic of monomer emission.

To explore the thermal properties and phase behavior of DGEBA/UF/C18-RG systems, DSC studies were performed. In a first series of experiments, 100:25 (w/w) mixtures of DGEBA/UF comprising between 0 and 5% (w/w) dye were cured at 200 °C for 10 min. A comparison of the second heating scans of cured films (Figure 3a) reveals that all dye-containing materials display the same T_g as the neat epoxy resin (86 °C). This finding suggests that the addition of small amounts of the fluorescent dye does not affect the thermal properties of the epoxy coating. Keeping the dye concentration fixed at 1% (w/w), we also explored the influence of the curing time, temperature, and cross-linker concentration. Expectedly, T_g increases with the curing time until it plateaus after ∼45 min, at which time the samples are fully cured (Figures 3b and S1a−c in the Supporting Information). When the curing temperature was decreased to 180 °C, full curing was achieved only after 180 min; however, the ultimate T_g proved to be independent of the curing profile (see Figure S1d in the Supporting Information). Figure 3b shows further that the resin's T_g increases with the cross-linker content. This observation is consistent with the theoretical description and experimental results on cured epoxy resin in the literature (40, 48, 49).

We next undertook a detailed spectroscopic investigation of the thermooptical properties of the new dye-containing coatings. A series of annealing experiments were carried out to probe the thermally induced aggregation of dye molecules above T_g. The data provide important insights into aggregation kinetics, and the effect is useful for exploitation in time−temperature indicators. Coatings based on 100:25:3 (w/w/w) DGEBA/UF/C18-RG were cured for 10 min at 200 °C and quenched to room temperature. The samples were subsequently placed on a hot stage, and the optical properties were monitored by in situ PL spectroscopy as a function of the time and temperature. No significant changes were observed if the temperature was kept below T_g (see Figure S2 in the Supporting Information); this is consistent with the limited free volume and low molecular motion in this temperature regime. Raising the temperature to above T_g resulted in a significant and irreversible change of the resins' fluorescence color, suggesting that phase separation between dye molecules and epoxy polymers occurred as a result of sharply increased translational mobility at the onset of T_g. A typical data set is shown in Figure 4a, which displays the fluorescence spectra of 100:25:3 (w/w/w) DGEBA/UF/C18-RG coatings that had been cured for 10 min at 200 °C and were, after quenching, annealed for different times at 120 °C. The spectra show the expected change of the relative intensities of the monomer (I_M, 507 nm) and excimer (I_E, 644 nm (50)) emission as a function of the annealing time. The ratios I_M/I_E extracted from these and corresponding data sets (obtained at different annealing temperatures between 100 and 140 °C) were correlated with the annealing time, as shown in Figure 4b. A comparison between the experimental data and fits to eq 1 (Figure 4b) reveals that the aggregation kinetics of the investigated coatings is well described by a single-exponential function:

$$I_M/I_E = I_{M\infty}/I_{E\infty} + Ae^{-t/\tau} \qquad (1)$$

where $I_{M\infty}/I_{E\infty}$ is the intensity ratio of the emission of monomer and excimer after annealing to equilibrium, A and τ are constants representing the magnitude and rate of change in
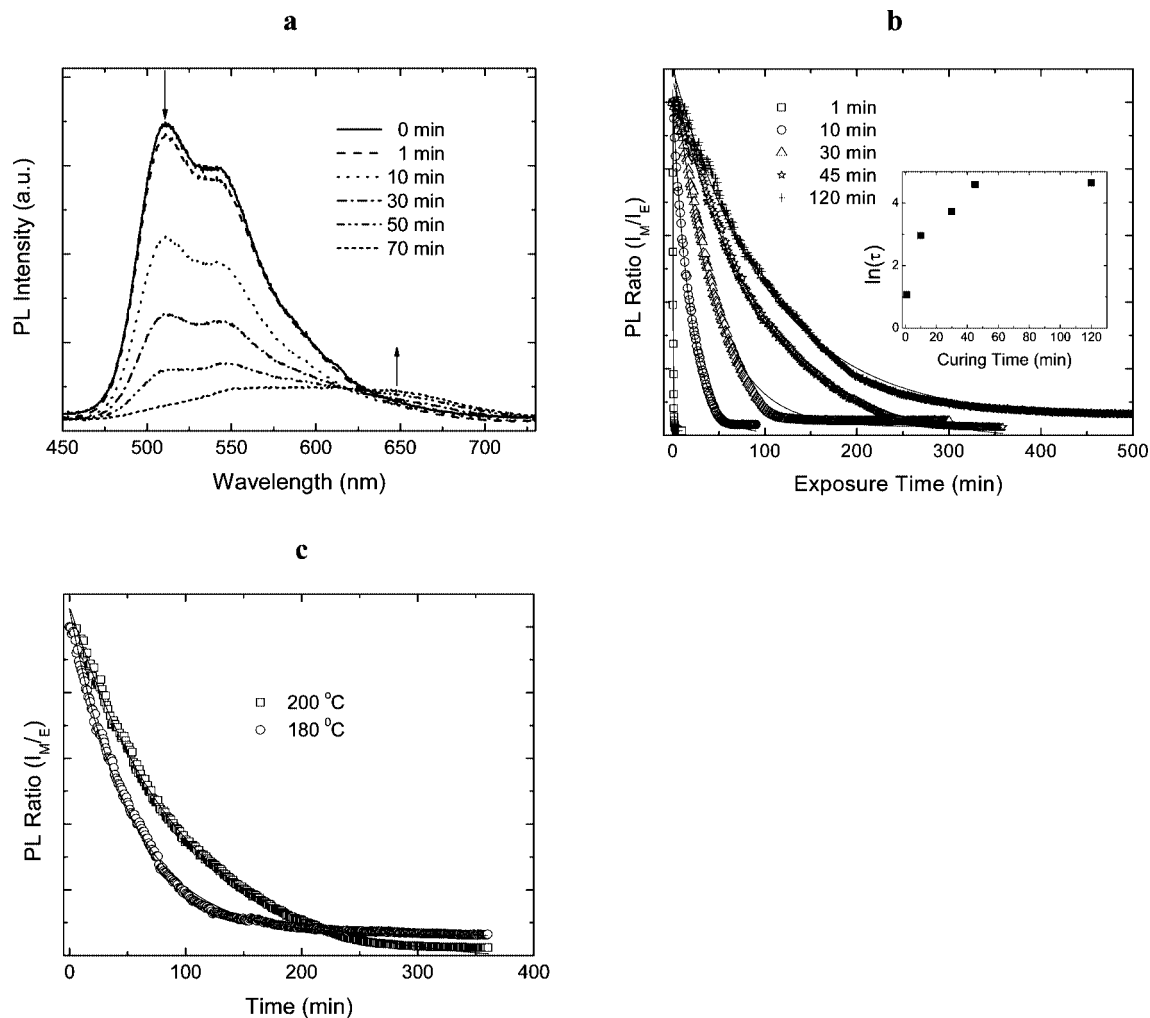
a

b

c

FIGURE 5. (a) Uncorrected PL emission spectra of 100:25:1 (w/w/w) DGEBA/UF/C18-RG coatings (cured for 10 min at 200 °C) as a function of the exposure time to ethanol at room temperature. Spectra were taken after 0−70 min. (b) Relative intensities of monomer-to-excimer emission I_M/I_E extracted from the spectra shown in part a as a function of the exposure time (○). Also shown are data obtained in a similar manner for the same composition cured at 200 °C for 1, 30, 45, and 120 min. Solid lines are least-squares fits according to eq 1. The inset displays a plot of $\ln(\tau)$, extracted from the fits shown in part b against the curing time. (c) I_M/I_E of 100:25:1 (w/w/w) DGEBA/UF/C18-RG coatings as a function of the exposure time in ethanol. The samples were fully cured at 180 °C (○, 180 min) or 200 °C (□, 45 min). Solid lines are least-squares fits according to eq 1.

I_M/I_E, and t is the annealing time. We have shown earlier that in blends with thermoplastic host polymers the aggregation rate constant τ follows an Arrhenius-type temperature dependence (31−36). As is evident from Figure 4c, which reveals a linear relationship between $\ln(\tau)$ and $1/T$ for 100:25:3 (w/w/w) DGEBA/UF/C18-RG coatings annealed at different temperatures, the coatings investigated here display the same behavior. Moreover, all other parameters being equal, the aggregation rate constant τ decreases if the dye concentration is reduced (Figure S3 in the Supporting Information). Thus, the aggregation process in the cross-linked epoxy/dye coatings investigated here appears to be predictable, and for a given composition, the fluorescence color of the material can be used to characterize its thermal history.

Expecting that swelling with liquid chemicals would result in a decrease of the epoxy coating's T_g and potentially cause irreversible aggregation of the dye molecules without increasing the temperature (36), we investigated the influence of chemical stimuli on the emission characteristics of the blend films. First experiments were conducted with 100:25:1 (w/w/w) DGEBA/UF/C18-RG coatings that were cured

for 10 min at 200 °C. Initially, i.e., after curing and quenching but before chemical exposure, these films displayed emission spectra that were dominated by monomer emission (Figure 5a). In situ PL spectroscopy revealed that the emission color changed gradually if the samples were immersed in *ethanol* (Figure 5a), indicative of phase separation and the formation of ground-state dye aggregates as a result of plasticization upon swelling with this solvent. At ambient temperature (21 ± 3 °C), the transition to an almost pure-red emission was accomplished in 1 h. A much faster response (full conversion in minutes) was observed upon exposure of the sample to MEK (Figure S4 in the Supporting Information), while immersion into water did not trigger any color changes in 8 h.

Because of its "intermediate character" (vide supra), ethanol was chosen as the stimulant for systematic kinetic studies. DSC experiments (Figure S5 in the Supporting Information) confirmed that swelling in ethanol indeed reduced T_g, although an accurate determination of the T_g
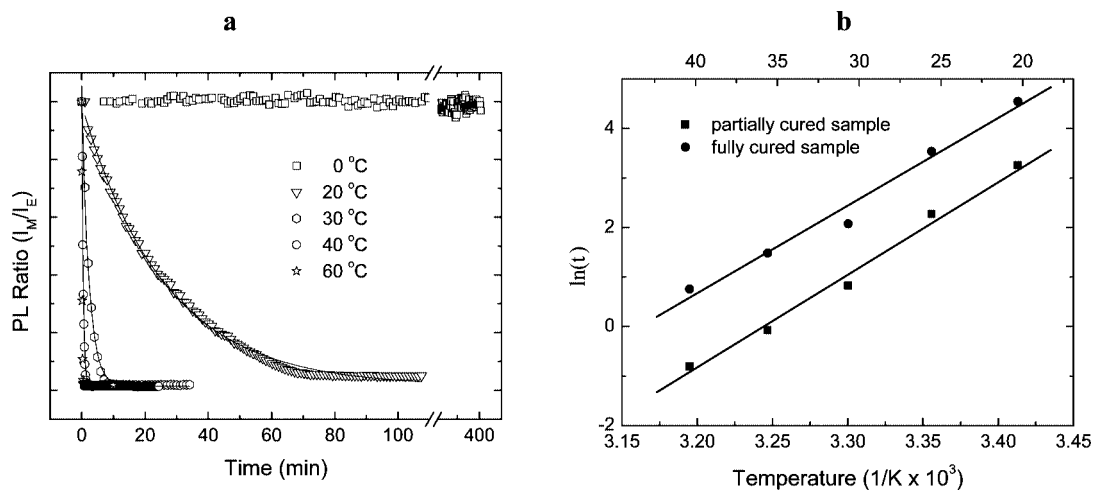
 Tang et al.

a

b

FIGURE 6. (a) Relative intensities of monomer-to-excimer emission I_M/I_E of 100:25:1 (w/w/w) DGEBA/UF/C18-RG coatings (cured for 10 min at 200 °C) as a function of the exposure time to ethanol at different temperatures. Solid lines are least-squares fits according to eq 1. (b) Plot of $\ln(\tau)$, extracted from the fits shown in part a against the inverse immersion temperature $1/T$ (■). Comparative data for fully cured coatings (cured for 45 min at 200 °C) are also shown (●).
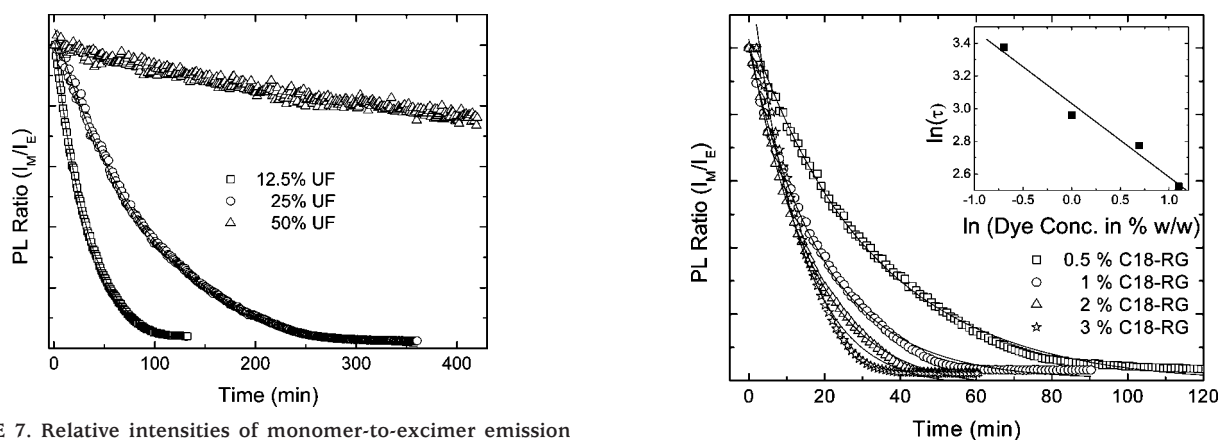

FIGURE 7. Relative intensities of monomer-to-excimer emission I_{507}/I_{644} of 100:XX:1 (w/w/w) DGEBA/UF/C18-RG coatings (cured for 60 min at 200 °C) as a function of the UF content XX and exposure time to ethanol at room temperature. Solid lines are least-squares fits according to eq 1.

FIGURE 8. Relative intensities of monomer-to-excimer emission I_M/I_E of 100:25:X (w/w/w) DGEBA/UF/C18-RG coatings (cured for 10 min at 200 °C) as a function of the dye content XX and exposure time to ethanol at room temperature. Solid lines are least-squares fits according to eq 1. The inset displays a plot of $\ln(\tau)$, extracted from the fits shown in the graph against the natutal logarithm of the dye concentration.

values at equilibrium swelling was stifled by the high volatility of ethanol. The I_M/I_E ratio of films immersed into ethanol (Figures 5b and S6 in the Supporting Information) shows that the aggregation kinetics, very much like the thermally induced aggregation discussed above, are well described by eq 1. Hypothesizing that the cross-link density (and the resulting differences in T_g) should exert a significant influence on the aggregation kinetics of the materials at hand, we next investigated the influence of the curing time by comparing the I_M/I_E traces of 100:25:1 (w/w/w) DGEBA/UF/C18-RG coatings that were cured for 1 (T_g = 75 °C), 10 (T_g = 86 °C), 30 (T_g = 98 °C), 45 (T_g = 114 °C), or 120 (T_g = 114 °C) min at 200 °C (Figure 5b) and which, after quenching, were immersed into ethanol at ambient temperature. Indeed, the aggregation rate constant τ increases with increasing T_g. Plots of $\ln(\tau)$ (inset in Figure 5b) and T_g (Figure 3b) versus the curing time are very similar, demonstrating that the effect is indeed related to T_g and that curing beyond the point where the T_g plateau has been reached has little effect on τ. The notion that the aggregation characteristics are largely governed by T_g is further supported by the fact

that 100:25:1 (w/w/w) DGEBA/UF/C18-RG coatings that were fully cured by different profiles (45 min at 200 °C or 180 min at 180 °C) display similar aggregation characteristics upon immersion into ethanol (Figure 5c).

We next investigated the temperature dependence of the chemically induced color changes of 100:25:1 (w/w/w) DGEBA/UF/C18-RG coatings (cured at 200 °C for 10 min) by immersing the coatings into ethanol at different temperatures in the regime between 0 and 60 °C. Figure 6a, which shows I_M/I_E as a function of the exposure time and temperature, reveals that the emission characteristics remained essentially unchanged over a period of 6 h if the coatings were immersed into ethanol at 0 °C. This suggests that, under these conditions, T_g is not sufficiently suppressed by swelling with ethanol to allow for dye aggregation. By contrast, increasing the exposure temperature to 20 °C triggered a PL color change from monomer-to-excimer emission that was complete after ca. 1 h; faster responses (minutes to seconds) were observed in the regime of 30−60
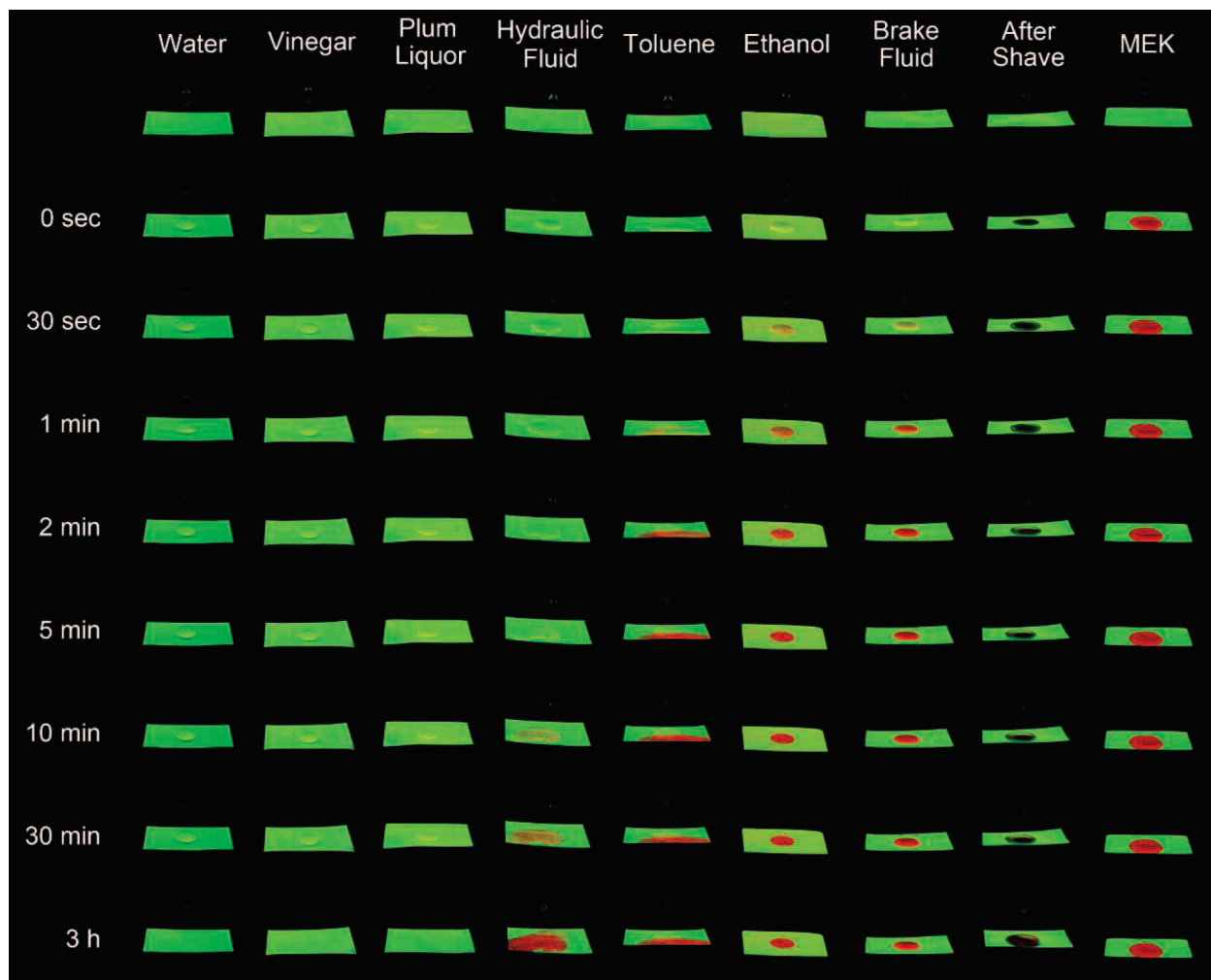
FIGURE 9. Pictures of 100:12.5:3 (w/w/w) DGEBA/UF/C18-RG coatings (cured for 1 min at 200 °C) on aluminum substrates as a function of the exposure time to different (household) chemicals that were dropped onto the coatings at room temperature. The samples are shown under illumination with UV light of a wavelength of 365 nm.

°C (Figure S7 in the Supporting Information). As for the purely thermally triggered aggregation (vide supra), the observed PL color changes were found to fit well to a single-exponential equation. As is evident from Figure 6b, which reveals a linear relationship between $\ln(\tau)$ and the inverse exposure temperature $1/T$, the Arrhenius-type activation behavior is maintained. Furthermore, control of τ via the cross-link density remains feasible, as evidenced by the increase of τ upon extending the curing time to 45 min (Figure 6b). Figure 7, which plots I_M/I_E of fully cured 100:XX:1 (w/w/w) DGEBA/UF/C18-RG coatings (cured for 60 min at 200 °C) as a function of the UF content XX and exposure time to ethanol at room temperature, demonstrates that the aggregation rate can also be tailored by controlling the cross-link density via the content of the UF cross-linker.

With reference to the fact that the chromophore content was found to exert a significant influence on the aggregation rate in thermoresponsive sensor systems (31−35), we also investigated this parameter in the context of ethanol-induced dye aggregation in DGEBA/UF/C18-RG resins. Coatings comprising DGEBA and UF in a 100:25 (w/w) ratio and between 0.5 and 3 % (w/w) C18-RG were cured for 10 min at 200 °C and quenched to ambient temperature. As discussed before

(Figure 3a), these coatings all have a similar T_g of ~86 °C, independent of the dye content. The I_M/I_E traces extracted from in situ PL experiments on samples immersed in room-temperature ethanol are shown as a function of the exposure time in Figure 8. As expected, the data reveal promoted aggregation between the C18-RG molecules upon increasing dye concentration. Interestingly, a plot of $\ln(\tau)$ (inset in Figure 8) versus the natural logarithm of the dye content reveals a linear relationship, demonstrating that it is possible to rationally control the aggregation rate via the dye concentration. In summary, our detailed kinetic study has shown that the color change of the dye-containing epoxy coatings upon exposure to a penetrating chemical is well described by standard kinetic models and can be minutely controlled via the chemical structure and cross-link density of the resin and the dye content.

In order to probe the usefulness of the responsive nature of the new epoxy resins as chemical sensors in different environments, we finally investigated the response of lightly cured (1 min at 200 °C) 100:12.5:3 (w/w/w) DGEBA/UF/C18-RG coatings of aluminum (Figure 9a) as well as glass (Figure S8 in the Supporting Information) upon exposure to a range of fluids that were selected to probe a broad spectrum of
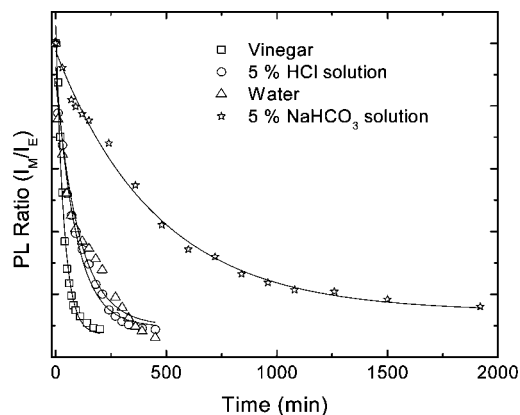
ACS APPLIED MATERIALS & INTERFACES VOL. 1 • NO. 3 • 688–696 • 2009 Tang et al. www.acsami.org

FIGURE 10. Relative intensities of monomer-to-excimer emission I_M/I_E of 100:12.5:3 (w/w/w) DGEBA/UF/C18-RG coatings (cured for 1 min at 200 °C) as a function of the exposure time to different solvents at 49 °C.

chemical stimulants. The low cross-link density (short curing time and low cross-linker content) and the high dye content [3 % (w/w)] bestow this composition with high responsiveness. Figure 9a provides a graphical summary of some of the experiments conducted at room temperature and highlights a number of interesting features. Clearly, the response shows at least some selectivity. At room temperature, the coatings are nonresponsive to highly polar substances or mixtures such as water, vinegar, and Swiss plum liquor [alcohol content 41 % (v/v)], indicative of a low degree of swelling and T_g reduction upon exposure. On the other hand, the fluorescence color changes instantaneously upon contact with MEK (dielectric constant = 18.4) or aftershave, indicating that solvents of intermediate polarity swell the resin particularly well. In the case of the aftershave, the color change appears to be not exclusively related to the excimer formation but the dye contained in the product appears to impart some color and to cause quenching of the C18-RG's fluorescence. Automotive brake fluid, ethanol, toluene, and aviation hydraulic fluid all lead to color changes, but the response times are clearly slower than those observed upon exposure to MEK or aftershave. Comparative examples on glass substrates (Figure S8 in the Supporting Information) demonstrate that the nature of the substrate does not significantly influence the response of the coatings (we surmise that minor differences may be related to slightly different curing conditions). In view of the temperature dependence observed upon exposure of the coatings to ethanol (vide supra), we surmised that a temperature increase would change the responsiveness of the coatings toward aqueous stimuli. Indeed, at 49 °C all water-based agents cause dye aggregation, as indicated by the appearance of red excimer emission. Figure 10 compares the aggregation kinetics from films immersed in water, vinegar, and 5 % aqueous solutions of HCl and NaHCO₃, respectively. The data fit well to the single-exponential functions with aggregation rate constants τ on the order of minutes (vinegar) to hours (NaHCO₃). The comparison reveals that, even for several aqueous systems, some selectivity is maintained. Acidic solutions display faster aggregation speed in comparison with water and basic solution, perhaps

because of the fact that epoxy coatings are susceptible to attack by acidic solvent especially acetic acid, which can, at least in part, form acetate salts with the amine group (41). The resulting hydrophilic ion pairs increase the solubility of water in the film and increase the permeability.

CONCLUSIONS

In summary, we developed a new concept for responsive thermoset coatings that are tailored to display significant, irreversible fluorescence color changes upon exposure to chemical and thermal stimuli. The materials investigated here were prepared by dissolving a chromogenic, fluorescent oligo(*p*-phenylenevinylene) dye into a cross-linked epoxy resin by reacting dye/monomer mixtures at high temperature and quenching the cured polymer below its glass transition temperature. Exposure of these materials to chemical solvents can decrease the materials' T_g through plasticization, which leads to aggregation of monomer to excimer. This response is well described by standard kinetic models and can be minutely controlled via the chemical structure and cross-link density of the resin and the dye content. In view of the design simplicity and easy read-out, the stimuli-responsive properties exhibited here by the investigated coating systems appear to bear a significant potential to visualize coating exposure before corrosion occurs. Further, the approach appears to be readily adaptable to other chemistries.

Supporting Information Available: DSC traces of DGEBA/UF/C18-RG resins (100:X:1, w/w/w) cured under different conditions; relative intensities of monomer-to-excimer emission, I_M/I_E of 100:25:3 (w/w/w) DGEBA/UF/C18-RG coatings annealed at 80 °C; I_M/I_E of 100:25:X (w/w/w) DGEBA/UF/C18-RG coatings annealed at 120 °C; I_M/I_E of 100:25:1 (w/w/w) DGEBA/UF/C18-RG coatings exposed to different solvents; DSC traces of 100:25:1 (w/w/w) DGEBA/UF/C18-RG coatings before and after immersion in ethanol; I_M/I_E of 100:25:1 (w/w/w) DGEBA/UF/C18-RG coatings as a function of the exposure time in ethanol; and I_M/I_E of 100:25:1 (w/w/w) DGEBA/UF/C18-RG coatings as a function of the exposure time in ethanol at different temperatures. This material is available free of charge via the Internet at http://pubs. acs.org.

REFERENCES AND NOTES

(1)   Leclerc, M. *Adv. Mater.* **1999**, *11*, 1491–1498.
(2)   Seeboth, A.; Lötzsch, D. In *Encyclopedia of Polymer Science and Technology*, 3rd ed.; Kroschwitz, J. I., Ed.; Wiley-Interscience: New York, 2003; Vol. 12, p 143.
(3)   Hamada, F. N.; Rosenzweig, M.; Kang, K.; Pulver, S. R.; Ghezzi, A.; Jegla, T. J.; Garrity, P. A. *Nature* **2008**, *454*, 217–220.
(4)   Balamurugan, S. S.; Bantchev, G. B.; Yang, Y.; McCarley, R. L. *Angew. Chem., Int. Ed.* **2005**, *44*, 4872–4876.
(5)   Beck, J. B.; Rowan, S. J. *J. Am. Chem. Soc.* **2003**, *125*, 13922–13923.
(6)   Wang, Y.; Archambault, N.; Marold, A.; Weng, L.; Lucht, B. L.; Euler, W. B. *Macromolecules* **2004**, *37*, 5415–5422.
(7)   van den Berg, O.; Sengers, W. G. F.; Jager, W. F.; Picken, S. J.; Wübbenhorst, M. *Macromolecules* **2004**, *37*, 2460–2470.

(8) Lu, Y.; Yang, Y.; Sellinger, A.; Lu, M.; Huang, J.; Fan, H.; Huddad, R.; Lopez, G.; Burns, A. R.; Sasaki, D. Y.; Shelnutt, J.; Brinker, C. J. *Nature* **2001**, *410*, 913–917.

(9) Lee, S. B.; Koepsel, R. R.; Russel, A. J. *Nano Lett.* **2005**, *5*, 2202–2206.

(10) Nallicheri, R. A.; Rubner, M. F. *Macromolecules* **1991**, *24*, 517–525.

(11) Edrington, A. C.; Urbas, A. M.; DeRege, P.; Chen, C. X.; Swager, T. M.; Hadjichristidis, N.; Xenidou, M.; Fetters, L. J.; Joannopoulos, J. D.; Fink, Y.; Thomas, E. L. *Adv. Mater.* **2001**, *13*, 421–425.

(12) Lawrence, J. R.; Shim, G. H.; Jiang, P.; Han, M. G.; Ying, Y.; Foulger, S. H. *Adv. Mater.* **2005**, *17*, 2344–2349.

(13) Natansohn, A.; Rochon, P. *Chem. Rev.* **2002**, *102*, 4139–4175.

(14) Shibaev, V.; Bobrovsky, A.; Boiko, N. *J. Photochem. Photobiol. A* **2003**, *155*, 3–19.

(15) Wigglesworth, T.; Myles, A. J.; Branda, N. R. *Eur. J. Org. Chem.* **2005**, 1233–1238.

(16) Albert, K. J.; Lewis, N. S.; Schauer, C. L.; Sotzing, G. A.; Stitzel, S. E.; Vaid, T. P.; Walt, D. R. *Chem. Rev.* **2000**, *100*, 2595–2626.

(17) McQuade, D. T.; Pullen, A. E.; Swager, T. M. *Chem. Rev.* **2000**, *100*, 2537–1574.

(18) Potyrailo, R. A. *Angew. Chem., Int. Ed.* **2006**, *45*, 702–723.

(19) Thomas, S. W., III; Joly, G. D.; Swager, T. M. *Chem. Rev.* **2007**, *107*, 1339–1386.

(20) Basabe-Desmonts, L.; Reinhoudt, D. N.; Crego-Calama, M. *Chem. Soc. Rev.* **2007**, *36*, 993–1017.

(21) Chen, Y.; Thakar, R.; Snee, P. T. *J. Am. Chem. Soc.* **2008**, *130*, 3744–3745.

(22) Wang, F.; Gu, H.; Swager, T. M. *J. Am. Chem. Soc.* **2008**, *130*, 5392–5393.

(23) Palazzotto, M. C.; Rakow, N. A.; Wendland, M. S. U.S. Patent Application 20080070320, 2008.

(24) Jenekhe, S. A.; Kiserow, D. I. *Chromogenic Phenomena in Polymers*; ACS Symposium Series 888; American Chemical Society: Washington, DC, 2005; p 2.

(25) Löwe, C.; Weder, C. *Adv. Mater.* **2002**, *14*, 1625–1629.

(26) Crenshaw, B. R.; Weder, C. *Macromolecules* **2006**, *39*, 9581–9589.

(27) Crenshaw, B. R.; Burnworth, M.; Khariwala, D.; Hiltner, A.; Mather, P. T.; Simha, R.; Weder, C. *Macromolecules* **2007**, *40*, 2400–2408.

(28) Crenshaw, B. R.; Weder, C. *Chem. Mater.* **2003**, *15*, 4717–4724.

(29) Kunzelman, J.; Kinami, M.; Crenshaw, B. R.; Protasiewicz, J.; Weder, C. *Adv. Mater.* **2008**, *20*, 119–122.

(30) Crenshaw, B. R.; Kunzelman, J.; Sing, C. E.; Ander, C.; Weder, C. *Macromol. Chem. Phys.* **2007**, *208*, 572–580.

(31) Kinami, M.; Crenshaw, B. R.; Weder, C. *Chem. Mater.* **2006**, *18*, 946–955.

(32) Kunzelman, J.; Crenshaw, B. R.; Kinami, M.; Weder, C. *Macromol. Rapid Commun.* **2006**, *27*, 1981–1987.

(33) Crenshaw, B. R.; Weder, C. *Adv. Mater.* **2005**, *17*, 1471–1476.

(34) Kunzelman, J.; Chung, T.; Mather, P. T.; Weder, C. *J. Mater. Chem.* **2008**, *18*, 1082–1086.

(35) Sing, C. E.; Kunzelman, J.; Weder, C. *J. Mater. Chem.* **2009**, *19*, 104.

(36) Kunzelman, J.; Crenshaw, B. R.; Weder, C. *J. Mater. Chem.* **2007**, *17*, 2989–2991.

(37) Donati, F.; Pucci, A.; Cappelli, C.; Mennucci, B.; Ruggeri, G. *J. Phys. Chem. B* **2008**, *112*, 3668–3679.

(38) Pucci, A.; Cuia, F. D.; Signori, F.; Ruggeri, G. *J. Mater. Chem.* **2007**, *17*, 783–790.

(39) Pucci, A.; Cappelli, C.; Bronco, S.; Ruggeri, G. *J. Phys. Chem. B* **2006**, *110*, 3127–3134.

(40) Pucci, A.; Bertoldo, M.; Bronco, S. *Macromol. Rapid Commun.* **2005**, *26*, 1043–1048.

(41) Wicks, Z. W.; Jones, F. N.; Pappas, S. P.; Wicks, D. A. *Organic Coatings: Science and Technology*, 3rd ed.; John Wiley & Sons, Inc.: Hoboken, NJ, 2007.

(42) *Epoxy Resins: Chemistry and Technology*; May, C. A., Ed.; Dekker: New York, 1976; p 485.

(43) Löwe, C.; Weder, C. *Synthesis* **2002**, *9*, 1185–1190.

(44) Freudenmann, R.; Behnisch, B.; Hanack, M. *J. Mater. Chem.* **2001**, *11*, 1681–1686.

(45) Flory, P. J. *Principles of Polymer Chemistry*; Cornell University Press: Ithaca, NY, 1953, p 47.

(46) Gee, G. The Thermodynamic Study of Rubber Solutions and Gels. In *Advances in Colloid Science*; Mark, H., Whitby, G. S., Eds.; Interscience: New York, 1946; Vol. II, p 145.

(47) Because of a K → LC transition (ref 31), C18-RG dye does not display any excimer emission above 142 °C. Therefore, the employed methodology does not allow one to ascertain the solubility limit of compositions with dye concentrations of >2 % (w/w). However, the available data allow us to extrapolate that blends comprising 3 % (w/w) of the dye do indeed satisfy the required solubility profile.

(48) Potter, W. G. *Epoxide Resins*; Butterworth & Co.: London, 1970; p 37.

(49) Lee, H.; Neville, K. *Epoxy Resins: Their Application and Technology*; McGraw-Hill Book Company, Inc.: New York, 1957; p 52.

(50) Note that the spectra recorded in situ are uncorrected; as a result, the intensities of the red portions of the spectra are suppressed.